Choosing the Right Reagent for the Determination of the Absolute Configuration of Amines by NMR: MTPA or MPA?†

J. M. Seco, Sh. K. Latypov,‡ E. Quiñoá, and R. Riguera*

Departamento de Química Orgánica, Facultad de Química, and Instituto de Acuicultura, Universidad de Santiago de Compostela, 15706, Santiago de Compostela, España, FAX 34-81-591091

Received March 7, 1997[⊗]

Molecular mechanics, semiempirical (AM1), aromatic shielding effect calculations, and dynamic NMR experiments demonstrate that MTPA amides are constituted by three main conformers, sp, ap3, and ap1 due to restricted rotation around the C_α−CO and the C_α−Ph bonds. Unlike MTPA esters, where the three rotamers have almost identical populations, in MTPA amides rotamer sp is more populated than the other two and has a shielding rather than deshielding character. This produces larger $\Delta\delta^{RS}$ values for MTPA amides than for MTPA esters. Therefore, inference of absolute configuration with this reagent should be correspondingly more reliable for amines than for alcohols. Assignment of absolute configuration of chiral primary α-substituted amines with MTPA gives similar $\Delta\delta^{RS}$ values than with MPA. A graphical description of the aromatic magnetic field distribution in MTPA and MPA amides, and its use to correlate the average chemical shifts with the absolute configuration of the amine, is presented.

Introduction

Methoxy(trifluoromethyl)phenylacetic acid (MTPA, Mosher's reagent, **1**) and methoxyphenylacetic acid (MPA, **2**) are two frequently used reagents for determination of the absolute configuration of alcohols and amines by NMR. The method is based on the derivatization of the substrate with the two enantiomers of the chiral reagent and comparison of the chemical shifts of the resulting diastereomers.[1]

Figure 1 illustrates the different influence of the phenyl ring on the NMR signals of L_1 and L_2 in the (*R*)- and (*S*)-MTPA amides. The difference[2] $\Delta\delta^{RS} = \delta^R - \delta^S$ can be used to deduce the location of L_1 and L_2 and thus, the absolute configuration at the chiral center. Since the method is based on the influence of the aromatic ring on the substrate substituents, the precise geometry and orientation of the phenyl group in relation to the "substrate amine" part of the molecule and the relative population of the conformers are essential to define the degree of confidence of the prediction.

In the case of secondary alcohols, new more efficient reagents than MTPA and MPA,[3a,b] and more suitable conditions for the NMR experiments,[3c] have been developed. However, no great improvement was observed when these new reagents were used in the determination of the absolute configuration of primary amines.[3d]

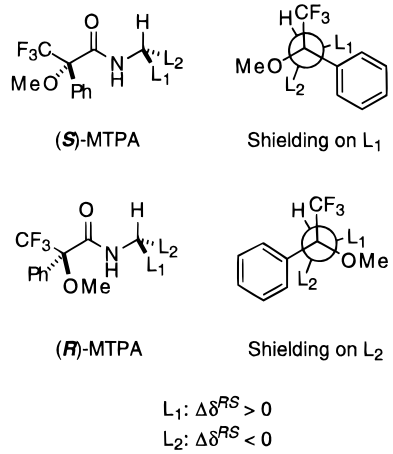

Figure 1. NMR conformational model for MTPA amides.[1a]

We recently described the limitations of MTPA (**1**) as a reagent for the determination of the absolute stereochemistry of alcohols[3e] and pointed out the complexity of the conformational composition of the MTPA esters (three conformers with similar populations). This is further complicated by the different orientations shown by the phenyl ring. In some conformers the aromatic ring produces shielding and in others deshielding on the same ligand of the alcohol moiety. As a result, the $\Delta\delta^{RS}$ absolute values observed in MTPA esters are smaller and the assignment of the absolute configuration is less reliable than those recorded with MPA esters.

In this paper we show that MTPA is a reliable reagent, comparable to MPA, for the determination of the absolute configuration of primary α-substituted amines. We have used molecular mechanics and semiempirical calculations to predict the conformational composition of MTPA amides and compared these data with those obtained from aromatic shielding effect calculations[4] and experi-

† For a previous report on the use of these reagents with secondary alcohols, see ref 3e.

‡Present address: The Institute of Organic & Physical Chemistry of Russian Academy of Sciences, Kazan, 420083, Tatarstan, the Russian Federation.

⊗ Abstract published in *Advance ACS Abstracts,* October 1, 1997.

(1) (a) Sullivan, G. R.; Dale, J. A.; Mosher, H. S. *J. Org. Chem.* **1973**, *38*, 2143−2147. (b) Trost, B. M.; Belletire, J. L.; Goldleski, P. G.; McDougal, P. G.; Balkovec, J. M.; Baldwin, J. J.; Christy, M. E.; Ponticello, G. S.; Varga, S. L.; Springer, J. P. *J. Org. Chem.* **1986**, *51*, 2370−2374. (c) For a review see: Uray, G. In *Houben-Weyl Methods in Organic Chemistry*; (Helchen, G., Hoffmann, R. W., Mulzer, J., Schaumann, E., Eds.; Thieme: Stuttgart, 1996, Vol. 1, p 253. Eliel, E. L.; Wilen, S. H.; Mander, L. N. *Stereochemistry of Organic Compounds*; Wiley-Interscience: New York, 1994.

(2) For a given proton of a parent alcohol or amine, $\Delta\delta^{RS}$ is the difference in the chemical shifts between (*R*)-MTPA (or (*R*)-MPA) and (*S*)-MTPA (or (*S*)-MPA) derivatives.

(3) (a) Latypov, Sh. K.; Seco, J. M.; Quiñoá, E.; Riguera, R. *J. Org. Chem.* **1995**, *60*, 504−515. (b) Seco, J. M.; Latypov, Sh. K.; Quiñoá, E.; Riguera, R. *Tetrahedron Lett.* **1994**, *35*, 2921−2924. (c) Seco, J. M.; Latypov, Sh. K.; Quiñoá, E.; Riguera, R. *Tetrahedron Asymmetry* **1995**, *6*, 107−110. (d) Latypov, Sh. K.; Seco, J. M.; Quiñoá, E.; Riguera, R. *J. Org. Chem.* **1995**, *60*, 1538−1545. (e) Latypov, Sh. K.; Seco, J. M.; Quiñoá, E.; Riguera, R. *J. Org. Chem.* **1996**, *61*, 8569−8577.

(4) Haigh, C. W.; Mallion, R. B. *Progress in NMR Spectroscopy*; Pergamon Press, Ltd.: New York, 1980; Vol. 13, pp 303−344.

S0022-3263(97)00427-1 CCC: $14.00

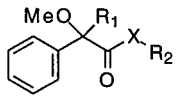

X	R_1	R_2	Compound[5]
O	CF_3	H	MTPA, **1**
O	H	H	MPA, **2**
NH	CF_3	methyl	**3**
NH	H	methyl	**4**
NH	CF_3	(+)-bornyl	**5**
NH	H	(+)-bornyl	**6**
NH	CF_3	L-valine methyl ester	**7**
NH	H	L-valine methyl ester	**8**
NH	CF_3	L-leucine methyl ester	**9**
NH	H	L-leucine methyl ester	**10**
NH	CF_3	L-phenyl alanine methyl ester	**11**
NH	H	L-phenyl alanine methyl ester	**12**
NH	CF_3	L-tryptophan methyl ester	**13**
NH	H	L-tryptophan methyl ester	**14**
NH	CF_3	L-isoleucine methyl ester	**15**
NH	CF_3	L-methionine methyl ester	**16**
NH	CF_3	L-serine methyl ester	**17**
NH	CF_3	L-threonine methyl ester	**18**
NH	CF_3	L-isoleucinol	**19**
NH	CF_3	L-phenylalaninol	**20**
O	H	(-)-bornyl	**21**

Figure 2.

mental dynamic NMR, as well as a full set of experimental data with amines of known stereochemistry (Figures 2 and 3).

Calculations

To investigate the structure and number of the major conformers of MTPA amides, we resorted to MM for geometry minimization and to semiempirical AM1 calculations for energy assessment on the MTPA amide of methylamine (**3**) as the simplest model (Table 1). These results predict that rotation around the CO−NH bond generates, as expected, *E* and *Z* isomers, and that the *E* is higher in energy than the corresponding *Z* isomer. Consideration of rotations around the C_α−Ph and C_α−CO bonds leads to three lower energy rotamers in conformational equilibrium (sp_1, ap_1 and ap_3, Figure 4a). The sp rotamer is defined by the synperiplanar conformation of the C_α−CF_3 and C=O groups while the two ap rotamers have those two groups in an antiperiplanar disposition.[6] The difference between the two ap rotamers lies on the orientation of the phenyl ring plane with respect to rotation about the C_α−Ph bond. In ap1, the phenyl plane is near coplanar with the C_α−OMe bond, while in ap3 the phenyl ring and the C_α−CF_3 bond are nearly coplanar. Energy data indicate that sp-*Z* is the most stable rotamer, predominating over the other two ap ones which are higher in energy by ca. 0.5 and 0.9 kcal/mol, respectively.

Careful examination of these conformations (Figure 4) shows that shielding and deshielding effects on L_1/L_2 can be predicted from the location and orientation of the aryl ring plane in each conformer, as in the case of MTPA esters.[3d] For example, in the (*S*)-MTPA amide (Figure 5a), substituent L_2 is deshielded by the aromatic ring in rotamer ap_1, while shielded in ap_3, the predicted ap1 and ap3 populations being nearly identical (Table 1). Therefore, L_2 remains largely unaffected by the aromatic ring. In the (*R*)-MTPA amide, the anisotropic effect on L_2 in conformer sp (Figure 5b) produces a net shielding effect. Thus, the $\Delta\delta^{RS}$ value for L_2 is predicted to be negative for the absolute configuration shown in Figure 5 (and positive for L_1).

Unlike MTPA esters,[3e] where the three dominant rotamers have almost identical populations and opposing shielding/deshielding influences, in the MTPA amides rotamer sp is more populated than the other two and has shielding character. This strongly suggests that the $\Delta\delta^{RS}$ values should be larger for MTPA amides than for MTPA esters and their signs more reliable, and, consequently, inference of absolute configuration with this reagent should be more reliable for amines than for alcohols.

Comparison of the conformational composition of MTPA amides with that of MPA amides[3d] shows that MPA amides are constituted by just two main conformers, ap and the less stable sp (Figure 6). For instance, L_2 is shielded in both the (*S*)- and the (*R*)-MPA derivative and thus the difference $\Delta\delta^{RS}$ is correspondingly smaller than in MTPA amides. In addition, the predominant orientation of the phenyl ring in MTPA amides is more favorably oriented (by ca. 60°; see Figure 4) to shield the L_1/L_2 substituents than in MPA amides. In fact, the Ph ring in the sp conformer of MTPA amides is coplanar to the C_α−OMe bond while in MPA amides is coplanar to the C_α−H. The combination of these two factors might suggests that stronger shielding effects could be operative in MTPA than in MPA amides.

Dynamic NMR

The predominance of conformer sp deduced from the calculations suggests that dynamic NMR could be an excellent method to demonstrate experimentally the above predictions. We selected the (*R*)- and (*S*)-MTPA amides of (+)-bornylamine ((*R*)-**5** and (*S*)-**5**) as suitable compounds for dynamic NMR studies because **5** presents several hydrogens at different but very well defined locations relative to the phenyl ring. Confidence that experimental data on (*R*)-**5** and (*S*)-**5** can be safely interpreted on the light of our previous predictions was obtained from AM1 calculations. Table 2 shows that the number, type, and relative stabilities of the conformers

(5) (a) For simplification purposes and in coherence with previous papers (see ref 3), we will refer to these compounds by (*R*/*S*)-*n*, where (*R*/*S*) indicates the configuration at the chiral center of the auxiliary reagent (MPA or MTPA) and *n* is the digit that identifies the parent alcohol or amine. (b) For data on compounds **8**, **10**, **12**, and **14**, see reference 3d; for compounds **7**, **9**, **11**, **13**, **15**−**20**, see: Kusumi, T.; Fukushima, T.; Ohtani, I.; Kakisawa, H. *Tetrahedron Lett.* **1991**, *32*, 2939−2942; for compound **21** see reference 3e.

(6) It is important to note that conformer sp in a MTPA derivative corresponds to conformer ap in the MPA analogue, and *vice versa:* with MTPA, CF_3 and C=O are the groups taken as references to define the ap/sp relationship, while OMe and C=O are the ones taken with MPA.

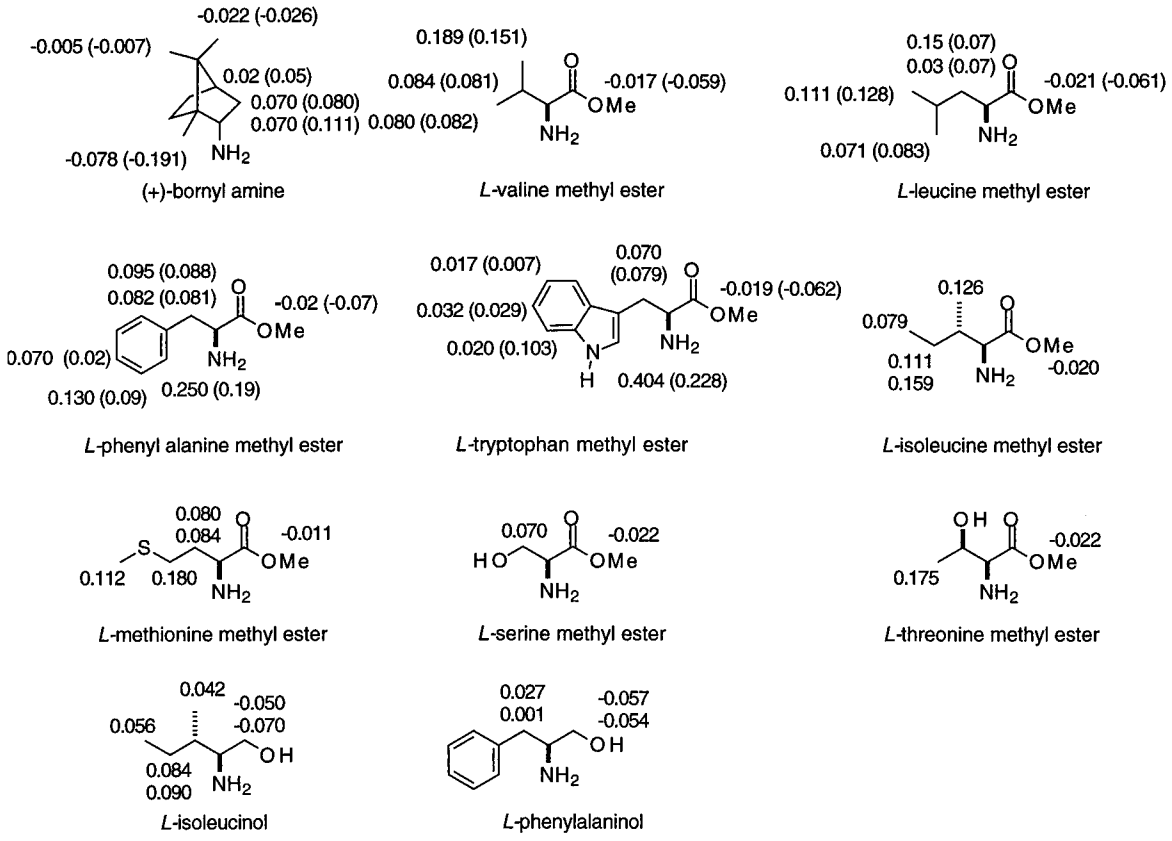

Figure 3. Selected $\Delta\delta^{RS}$ values (ppm, $CDCl_3$) of the (*R*)- and (*S*)-MTPA amides of the illustrated amines. For comparison purposes, MPA values are shown between brackets.[5b]

Table 1. Calculated AM1 Energies and Dipole Moments for the Main Conformers of the MTPA Amide of Methylamine (3)

conformer	ΔE (AM1) cal mol^{-1}	μ, D	Ph ring coplanar with
sp-*Z*	0.00	4.63	OMe
sp-*E*	2.08	5.18	OMe
ap_1-*Z*	0.51	1.60	OMe
ap_3-*Z*	0.43	2.38	CF_3
ap-*E*	5.19	3.27	CF_3

generated by amides (*R*)-**5** and (*S*)-**5** are coincident with those calculated for the simplest model (**3**) (Table 1).

Figure 7 presents the structures of the three (*R*)-**5** conformers, sp, ap_3, and ap_1, with sp as the most stable one. The latter has the aromatic shielding cone oriented toward Me(8′), Me(9′), and Me(10′), while in the other two conformers, the phenyl ring affects the other side of the bornyl skeleton, i.e. H(6′e). The different orientation of the Ph ring plane in the ap conformers, converts ap_3 in a shielding-producing form while ap_1 is a deshielding one. Due to the higher abundance of ap_3, the overall result should be a slight shielding that is, in fact, experimentally observed.

If the composition and structures shown in this scheme are correct, NMR should show all the hydrogens that are in the sp conformer under the shielding cone of the Ph ring (i.e. Me(10′)), undergoing greater shielding at lower temperatures due to the increase of the sp population, while those located in the other side of the molecule (i.e. H(6′e)) should move to upfield due to the ap3 increase. In fact, the NMR spectra of (*R*)-**5**, recorded at temperatures between 298 and 173 K (Table 3), corroborated the above predictions. The upfield shifts of Me(8′), Me(9′), and Me(10′) and the slight upfield movement of the H(6′e) signal were observed when the temperature of the NMR probe was decreased.

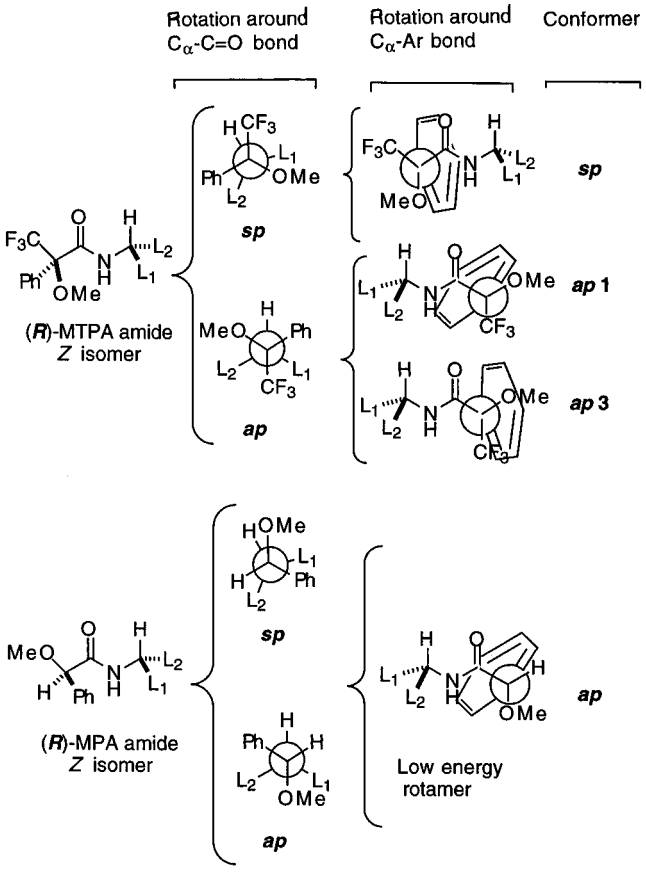

Figure 4. The lowest energy conformations of (*R*)-MTPA and (*R*)-MPA amides. Newman projections along the C_α−CO bond (sp and ap conformers) and C_α−Ph bond (sp, ap_1, and ap_3).

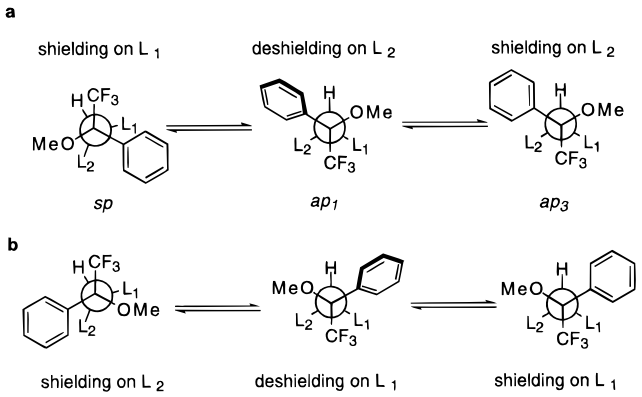

Figure 5. Low energy conformations of (a) (*S*)-MTPA and (b) (*R*)-MTPA *N*-methylamides, as obtained by MM and AM1.

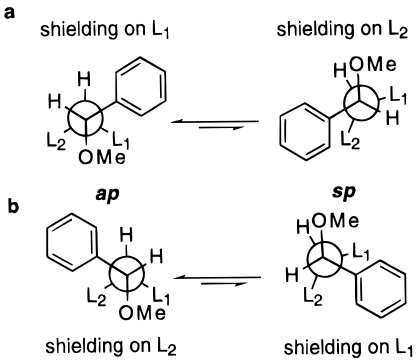

Figure 6. Low energy conformations of (a) (*S*)-MPA and (b) (*R*)-MPA *N*-methylamides, as obtained by MM and AM1.[3d]

Table 2. AM1 Energies and Aromatic Ring Anisotropy Increments[a] ($\Delta\sigma$) Calculated for the Low Energy Conformers of the (*R*)- and (*S*)-MTPA Amides of (+)-Bornylamine (5)

config	confor	ΔE (kcal/mol)	$\Delta\sigma$(6e)	$\Delta\sigma$(9/10)
(*R*)	sp-*E*	**3.20**	1.7	
(*R*)	sp-*Z*	**0.00**	0.0/0.1	
(*R*)	ap-*E*	**7.31**	0.0/1.0	
(*R*)	ap_1-*Z*	**0.61**		
(*R*)	ap_3-*Z*	**0.44**	0.2	
(*S*)	sp-*E*	**3.59**	0.2/0.7	
(*S*)	sp-*Z*	**0.00**	0.1	
(*S*)	ap-*E*	**7.71**	1.9	0.4/0.0
(*S*)	ap_1-*Z*	**0.66**		
(*S*)	ap_3-*Z*	**0.70**		

[a] Calculated by semiclassical model (see reference 4)

Similar predictions were confirmed experimentally for the (*S*)-**5** amide (Table 3). Thus, the signal due to H(6′e) is shielded by the aromatic ring in conformer sp, and those of Me(8′), Me(9′), and Me(10′) are shielded in ap_3 and deshielded in ap_1. As the predominant conformer is sp, H(6′e) is more strongly shielded in (*S*)-**5** than in (*R*)-**5**, while Me(8′), Me(9′), and Me(10′) are more shielded in (*R*)-**5** than in (*S*)-**5**.

An evaluation of the magnitude and importance of these shielding/deshielding effects can be obtained by comparison of the chemical shifts observed for selected protons of (*R*)-**5** and (*S*)-**5** with those of model compounds, with similar structure and well known orientation of the Ph ring.[3e] Suitable models are the (*R*)- and (*S*)-MPA esters of (−)-borneol (**21**) that, at low temperature (183 K), are constituted almost exclusively by a single rotamer (sp, Figure 8). In those conditions, the Ph ring produces no shielding effect on H(6′e) of (*R*)-**21**, nor on Me(8′), Me(9′), and Me(10′) of (*S*)-**21**, so the corresponding shifts

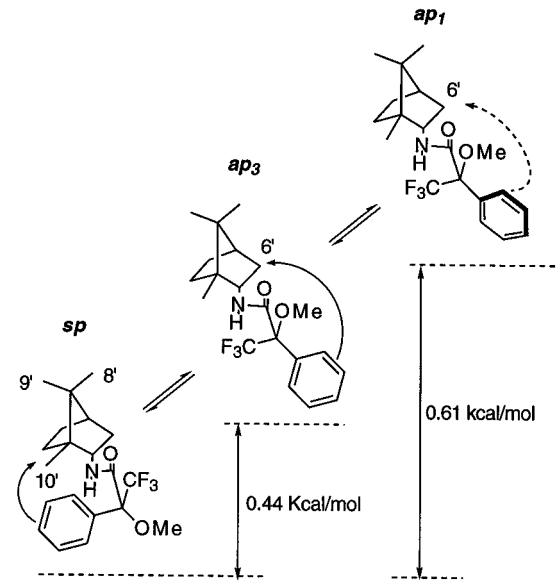

Figure 7. Low energy conformations of the (*R*)-MTPA amide of (+)-bornylamine ((*R*)-**5**). Plain arrows show shielding and dashed ones deshielding effects.

Table 3. Selected ^{1}H NMR Chemical Shifts of the (*R*)- and (*S*)-MTPA Amides of (+)-Bornylamine (5) (in ppm *vs* TMS; 4:1 CS_2/CD_2Cl_2)

config	*T*, K	H(6′e)	H(8′)	H(9′)	H(10′)
(*R*)	298	2.341	0.941	0.855	0.711
(*R*)	173	2.310	0.917	0.828	0.678
(*S*)	298	2.292	0.946	0.877	0.789
(*S*)	173	2.260	0.927	0.856	0.742

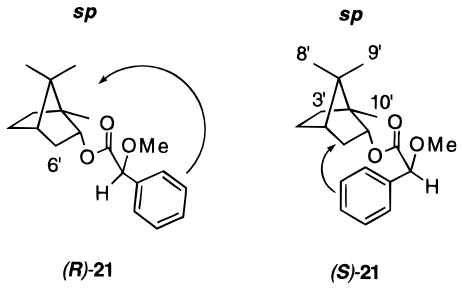

Figure 8. Low energy rotamers of (*R*)- and (*S*)-MPA esters of (−)-borneol (**21**). Shielding effects shown by arrows.

can be taken as reference. In fact, the difference between the chemical shifts of Me(8′), Me(9′), and Me(10′) in (*R*)-**5** and H(6′e) in (*S*)-**5**, with their counterparts in the spectra of (*R*)-**21**[7a] and (*S*)-**21**[7b] at 183 K, shows good general agreement with the calculated values (Table 2) and corroborates the finding of the small shielding predicted for those protons in (*R*)-**5** and (*S*)-**5**.

As temperature decreases below to 183 K, the NH signals in the spectra of (*R*)- and (*S*)-**5** first get broad and then split in two signals of unequal intensities due to the freezing of rotation around the NH−CO bond (*E*/*Z*). At those temperatures, rotation around the C_α−CO bond is still fast and shielded protons move further upfield. This confirms that sp is the predominant conformer and strongly suggests that intramolecular hydrogen bonds (CF_3/NH or OMe/NH) do not play a relevant role.

(7) (a) (*R*)-MPA ester of (*R*)-(+)-borneol (in CS_2 + CD_2Cl_2 4/1, T = 183 K): δ(6eq′) = 2.293. ppm δ(6ax′) = 0.948 ppm; (b) (*S*)-MPA ester of (*R*)-(+)-borneol (in CS_2 + CD_2Cl_2 4/1, T = 183 K): δ(10′) = 0.817 ppm.

(8) (a) Lee, M.; Lown, J. W. *J. Org. Chem.* **1987**, *52*, 5717−5721. (b) Mikolajczyk, M.; Kielbasinski, P. *Tetrahedron* **1981**, *37*, 233−284.

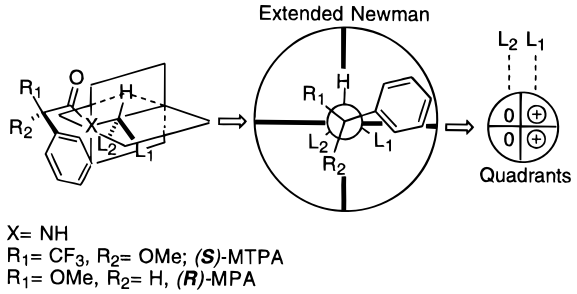

Figure 9. Spatial distribution of the magnetic field in MPA and MTPA amides.

Figure 3 shows the NMR experimental data of the MPA and MTPA amides of a selected number of amines of known absolute configuration (**5**−**20**).[5b] These examples were chosen because they present a large diversity of structural variations: hindered nonpolar cyclic frameworks, acyclic chains, presence of protic polar, nonpolar, and aromatic groups together with mixed combinations of the above. In spite of those differences, in all cases, the results fully agree with the ones already shown for (+)-bornylamine (**5**) and confirm the validity of the equilibrium compositions previously indicated.

Discussion

MPA and MTPA are so far the only commercially available chiral derivatizing agents for configuration assignment by NMR, and they have enjoyed widespread use.[3e] We have already predicted that in both MPA esters[3b] and amides,[3d] the aryl ring remains basically parallel to the C_α−H in the two main conformers (Figure 6), and, therefore, shielding is produced on L_1/L_2.

The spatial distribution[3e] of the magnetic field produced by the aromatic ring in a given conformer can be represented in graphical form as shown in Figure 9. Four quadrants are distinguished in the region of the asymmetric center of the substrate: (+) indicates shielding, (−) indicates deshielding, and (0) indicates no effect. Substituents L_1/L_2 will then be shifted in accordance with their position on a given sector, and the average shift will result from the position of L_1/L_2 in each conformer and consideration of the relative populations.

As shown in Figure 10a, in the (*R*)-MPA amide, L_1 is shielded (+) in conformer sp and unaffected (0) in ap, while in the (*S*)-MPA amide, L_1 is shielded (+) in ap and unaffected (0) in sp. As the ap rotamer is the predominant one, L_1 should be more shielded in the (*S*)- than in the (*R*)-MPA amide, and a positive $\Delta\delta^{RS}$ value should be obtained for this group. On the other hand, L_2 lies on the other side of the molecule, it is more shielded in the (*R*)- than in the (*S*)-MPA amide, and, as a consequence, it shows a negative $\Delta\delta^{RS}$ value.

The distribution of the aryl anisotropic field in (*R*)- and (*S*)-MTPA amides is illustrated in Figure 10b. The relative populations (p) and the spatial distribution of the aryl magnetic field of three conformers (two ap and one sp; see Figure 5) must be considered. Thus, in the (*R*)-MTPA amide, L_1 is located in the deshielding zone (−) in ap_1, in the shielding zone (+) in ap_3, and unaffected (0) in the sp rotamer. In the (*S*)-MTPA amide, L_1 is shielded (+) in sp and unaffected (0) in ap_1 and ap_3. In MTPA amides, the sp conformer is the most populated one, and, therefore, on average, L_1 should be more strongly shielded in the (*S*)-MTPA amide than in the (*R*)-MTPA amide ($\Delta\delta^{RS} > 0$). Substituent L_2 is located in the other side of the molecule and should be more shielded in the (*R*)- than in the (*S*)-MTPA amide ($\Delta\delta^{RS} < 0$).

Conclusions

It is known that MPA esters and amides are constituted by two main conformers, with different populations and characteristic aromatic field distributions.[3a,d] So, the prediction of the absolute configuration can be carried out with this reagent considering that the shielding conformer is the NMR relevant one.

The conformational composition and NMR contribution of each conformer to the average shifts are much more complicated in MTPA derivatives. This may lead, in the case of esters, to a risky configurational assignment[3e] because there is not a preferred conformer, and the Ph ring is not particularly well oriented to produce the strongest effect.

In the case of MTPA amides, a combination of two factors (the predominance of the shielding conformer sp and the better orientation of the phenyl ring plane) produces larger $\Delta\delta^{RS}$ values. Figure 11 shows the predicted average spectra of (a) (*R*)- and (*S*)-MPA amides and (b) (*R*)- and (*S*)-MTPA amides considering the contribution of every conformer and the resulting $\Delta\delta^{RS}$.

The model introduced by Mosher[2a] many years ago to predict the absolute configuration of amines is thus a simplified version of the conformational equilibrium shown in Figure 5 where the effects of the Ph ring on ap1 and ap3 are assumed to be more or less canceled, and conformer sp is considered to be the NMR relevant one. Therefore, MTPA and the classical model can be used to predict the absolute configuration of α-substituted primary amines.

In conclusion, the use of MTPA to determine the absolute configuration of amines has been based on the test of a fair number of amines of known absolute configuration. Our studies confirm the generality of those results and the signs and values of the $\Delta\delta^{RS}$ that are often comparable to the ones obtained with MPA: the population excess of one of the conformers and the excellent orientation of the phenyl ring in MTPA amides (Figure 3) allow a safe prediction of the absolute configuration.

Other arylmethoxyacetic acid reagents[3b] that have been proved to be much more effective than MPA and MTPA with alcohols produce no better separation of signals ($\Delta\delta^{RS}$ values) when applied to amines, and, therefore, both MTPA and MPA remain as the reagents of choice for this substrate.

Experimental Section

NMR Spectroscopy and Computational Methods. ^1H and ^{13}C NMR spectra of samples in 4:1 CS_2/CD_2Cl_2 (4 mg in 0.5 mL) were recorded at 500 and 250 MHz. Chemical shifts (ppm) are internally referenced to the TMS signal (0 ppm) in all cases. The NMR spectra were repeated at concentrations from ca. 8 mg/mL up to ca. 1 mg/mL to establish the absence of concentration effects. To ensure that cooling-heating cycles are reversible, ^1H NMR spectra were repeated at room temperature immediately after the low temperature experiments.

Molecular mechanics and semiempirical AM1 calculations were performed by the Insight II package. For additional information on NMR spectroscopy and computational methods see reference 3e.

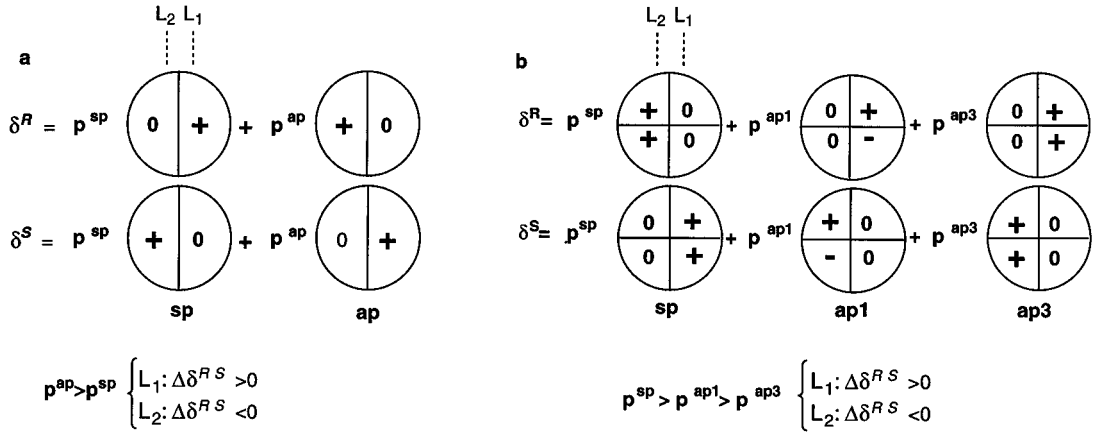

Figure 10. Distribution of shielding/deshielding effects for (a) MPA amides and (b) MTPA amides.

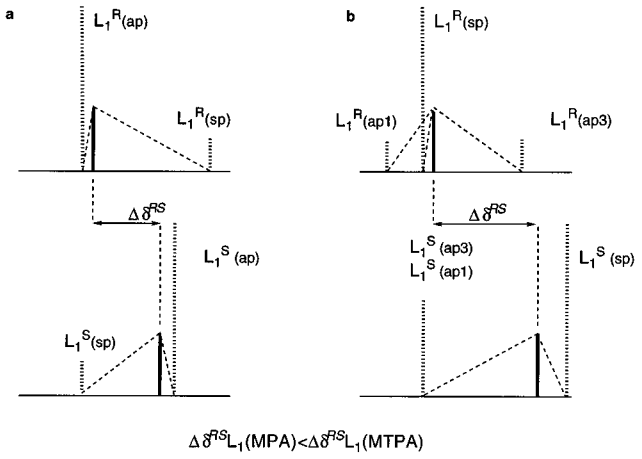

Figure 11. Predicted average ^{1}H NMR spectra of (a)MPA amides and (b) MTPA amides.

General. Preparation of diastereomeric amides from (+)-bornylamine and (*R*)- and (*S*)-2-methoxy-2-(trifluoromethyl)phenyl acetic acid was carried out with DCC.[8] The reaction mixture was filtered to remove the dicyclohexylurea, and the ester or amide was purified by flash chromatography on silica gel using dichloromethane as eluent. Further purification was accomplished by HPLC (μ-Porasil, 3 mm × 250 mm, hexane−ethyl acetate).

(+)-Bornyl (*S*)-2-methoxy-2-(trifluoromethyl)phenylacetamide ((*S*)-5). HPLC: t_R = 14.82 min (hexane−ethyl acetate, 96:4, 2 mL/min); [α] = −10.66 (*c* = 0.014, $CHCl_3$); ^{1}H NMR (500.13 MHz, $CDCl_3$) δ 4.47−4.45 (m, 2H), 7.35−7.31 (m, 3H), 6.72 (d, *J* = 8.3 Hz, 1H), 4.22 (dddd, *J* = 2.3, 4.5, 9.4, 11.3 Hz, 1H), 3.37 (s, 3H), 2.27 (m, 1 H), 1.71 (m, 1H), 1.60 (t, *J* = 4.5, 4.5 Hz, 1 H), 1.4−1.1 (m, 3 H), 0.87 (s, 3H), 0.81 (s, 3H), 0.80 (s, 3H), 0.70 (dd, *J* = 4.6, 13.35 Hz, 1H); ^{13}C NMR (62.9 MHz, $CDCl_3$) δ 13.5, 18.5, 19.7, 27.9, 28.3, 37.2, 44.8, 48.1, 49.7, 53.9, 55.0, 121.5, 126.2, 127.7, 128.5, 129.4, 132.7, 166.1; IR (NaCl): 3376, 2974, 2944, 1676, 1502, 1356, 1253; MS (E/I) *m*/*z* 369 (M^+). Anal. Calcd for $C_{20}H_{26}NO_2F_3$: C, 65.02; H, 7.09; N, 3.79. Found: C, 65.01; H, 7.10; N, 3.78.

(+)-Bornyl (*R*)-2-Methoxy-2-(trifluoromethyl)phenylacetamide ((*R*)-5). HPLC: t_R = 15.21 min (hexane−ethyl acetate, 96:4, 2 mL/min); [α] = −15.42 (*c* = 0.0035, $CHCl_3$); ^{1}H NMR (500.13 MHz, $CDCl_3$) δ 7.49−7.48 (m, 2H), 7.36−7.18 (m, 2H), 6.70 (d, *J* = 8.2 Hz, 1H), 4.22 (dddd, *J* = 2.3, 4.5, 9.4, 11.3 Hz, 1H), 3.37 (s, 3H), 2.32 (m, 1H), 1.71 (m, 1 H), 1.62 (t, *J* = 4.5, 4.5 Hz, 1H), 1.3−1.18 (m, 3 H), 0.87 (s, 3H), 0.80 (s, 3H), 0.77 (dd, *J* = 4.4, 13.4 Hz, 1H), 0.70 (s, 3H); ^{13}C NMR (62.9 MHz, $CDCl_3$) δ 13.7, 18.5, 19.6, 27.9, 28.2, 37.4, 44.8, 48.2, 49.6, 53.8, 54.9, 121.6, 126.2, 127.7, 128.5, 129.5, 132.9, 166.3; IR (NaCl): 3361, 2974, 2954, 2881, 1698, 1369, 1260; MS (E/I) *m*/*z* 369 (M^+). Anal. Calcd for $C_{20}H_{26}NO_2F_3$: C, 65.02; H, 7.09; N, 3.79. Found: C, 65.02; H, 7.07; N, 3.80.

Acknowledgment. This work was financially supported by CICYT (PM95-0135 and MAR95-33-CO2-O2) and the Xunta de Galicia (XUGA-20908B97 and 2090B96). We acknowledge the Spanish Ministry for Education and Science for a sabbatical research grant.

JO970427X